

## HNPS Advances in Nuclear Physics

Vol 18 (2010)

HNPS2010



### Neutral current neutrino- $^{94}\text{Mo}$ scattering in the context of the QRPA method

*K. G. Balasi, T. S. Kosmas*

doi: [10.12681/hnps.2535](https://doi.org/10.12681/hnps.2535)

#### To cite this article:

Balasi, K. G., & Kosmas, T. S. (2019). Neutral current neutrino- $^{94}\text{Mo}$  scattering in the context of the QRPA method. *HNPS Advances in Nuclear Physics*, 18, 31–36. <https://doi.org/10.12681/hnps.2535>

# Neutral current neutrino- $^{94}\text{Mo}$ scattering in the context of the QRPA method

K.G. Balasi and T.S. Kosmas

*Theoretical Physics Section, University of Ioannina, GR 45110 Ioannina, Greece*

## Abstract.

A systematic investigation of neutrino-nucleus reaction rates at low and intermediate energies of the stable  $^{94}\text{Mo}$  isotope is performed. Differential and integrated cross sections for neutrino inelastic scattering off the aforementioned target are calculated for neutrino energies  $\varepsilon_i \leq 100$  MeV. The nuclear wave functions for the initial and final nuclear states are constructed in the context of the quasi-particle random phase approximation (QRPA). The reliability of our method is tested by checking the reproducibility of the low-lying energy spectrum of the isotope under investigation.

**Keywords:** Semi-leptonic electroweak interactions; Neutrino-nucleus reactions; Inelastic cross sections; Quasi-particle random phase approximation

**PACS:** 23.40.Bw;25.30.Pt;21.60.Jz;26.30.+k

## INTRODUCTION

The interaction of neutrinos with nuclei both of charged and neutral current reactions, is a highly valuable source for detecting neutrino flavor and exploring the structure of electro-weak interactions [1, 2, 3, 4]. The determination of neutrino nucleus cross sections is of primary importance and to this aim various nuclear structure models have been employed for the description of the nuclear transition matrix elements. Among them the quasi-particle random phase approximation(QRPA) is offering reliable neutrino-nucleus reactions cross sections needed for current neutrino-detection experiments and star evolution modeling. Its main advantage lies in the ability to provide calculations based on a very large valence space.

Recently, an advantageous numerical approach has been developed for calculating the reduced matrix elements of neutrino induced nuclear transitions [5]. In the present work, we use this method to investigate inelastic neutrino scattering for neutral current reactions from stable  $^{94}\text{Mo}$  isotope at low and intermediate neutrino energies.

The starting point of our calculations is the Walecka-Donnelly formalism which describes in a unified way electromagnetic and weak semi-leptonic processes in nuclei, by taking advantage of the multipole decomposition of the relevant hadronic current density operators. This formalism has recently been improved, by constructing compact analytical expressions for all nuclear matrix elements of the basic multipole expansion operators entering these cross sections. The QRPA method employed for the construction of these nuclear states permits the evaluation of the individual contributions of the various incoherent (inelastic) neutrino induced nuclear transitions of the studied isotope [6].

## THE NEUTRINO-NUCLEUS FORMALISM

We consider neutral current neutrino-nucleus interactions in which a low and intermediate energy neutrino (or antineutrino) is scattered elastically or inelastically from a nucleus  $(A,Z)$ , via exchange of neutral  $Z^0$  bosons with the nucleus as

$$\nu_e + (A, Z) \longrightarrow \nu'_e + (A, Z)^* \quad (1)$$

where  $\nu_e$  ( $\bar{\nu}_e$ ) denote neutrinos (anti-neutrinos) of any flavor.

In the coherent channel, the nucleus remains in its ground state while in the incoherent the nucleus is excited. The neutrino-induced reactions leave the final nucleus in an excited state below or above particle-emission threshold.

The initial nucleus is assumed to be spherically symmetric and to reside in its ground state with angular momentum and parity  $J_p = 0^+$ . In our J-projected nuclear structure calculations, the initial and final nuclear states have well-defined spins and parities,  $|J_m^\pi\rangle$  (the index  $m$  counts the multipole state from low to high energies).

Then the differential cross section (according to the energy and the direction of the outgoing neutrino) is written as

$$\left( \frac{d^2\sigma_{i \rightarrow f}}{d\Omega d\omega} \right)_{\nu/\bar{\nu}} = \frac{G_F^2}{\pi} \frac{|\mathbf{k}_f| \varepsilon_f}{(2J_i + 1)} \left( \sum_{J=0}^{\infty} \sigma_{CL}^J + \sum_{J=1}^{\infty} \sigma_T^J \right) \quad (2)$$

where  $\omega = \varepsilon_i - \varepsilon_f$  is the excitation energy of the nucleus and  $\varepsilon_i$ , denotes the energy of the incoming neutrino while  $\varepsilon_f$  ( $\mathbf{k}_f$ ) represent the energy (momentum) of the outgoing lepton. The contributions  $\sigma_{CL}^J$ , for the Coulomb and Longitudinal components, and  $\sigma_T^J$ , for the transverse components, are written as

$$\begin{aligned} \sigma_{CL}^J &= (1 + \cos \Phi) \left| \langle J_f | \widehat{\mathcal{M}}_J(q) | J_i \rangle \right|^2 + (1 + \cos \Phi - 2b \sin^2 \Phi) \left| \langle J_f | \widehat{\mathcal{L}}_J(q) | J_i \rangle \right|^2 \\ &+ \left[ \frac{\omega}{q} (1 + \cos \Phi) \right] 2\Re \langle J_f | \widehat{\mathcal{L}}_J(q) | J_i \rangle \langle J_f | \widehat{\mathcal{M}}_J(q) | J_i \rangle^* \end{aligned} \quad (3)$$

$$\begin{aligned} \sigma_T^J &= (1 - \cos \Phi + b \sin^2 \Phi) \left[ \left| \langle J_f | \widehat{\mathcal{T}}_J^{mag}(q) | J_i \rangle \right|^2 + \left| \langle J_f | \widehat{\mathcal{T}}_J^{el}(q) | J_i \rangle \right|^2 \right] \\ &\mp \frac{(\varepsilon_i + \varepsilon_f)}{q} (1 - \cos \Phi) 2\Re \langle J_f | \widehat{\mathcal{T}}_J^{mag}(q) | J_i \rangle \langle J_f | \widehat{\mathcal{T}}_J^{el}(q) | J_i \rangle^* \end{aligned} \quad (4)$$

where  $\Phi$  is the lepton scattering angle and  $b = \varepsilon_i \varepsilon_f / q^2$ , In our convention ( $\hbar = c = 1$ ) it holds  $|\mathbf{k}_f| = \varepsilon_f$ . The summations in Eq. (2) contain the contributions of the well known operators Coulomb  $\widehat{\mathcal{M}}_J$ , longitudinal  $\widehat{\mathcal{L}}_J$ , transverse electric  $\widehat{\mathcal{T}}_J^{el}$  and transverse magnetic  $\widehat{\mathcal{T}}_J^{mag}$  multipole operators as defined in [6].

The magnitude of the three momentum transfer  $q$  is given by

$$q = |\mathbf{q}| = [\omega^2 + 2\varepsilon_i \varepsilon_f (1 - \cos \Phi)]^{\frac{1}{2}} \quad (5)$$

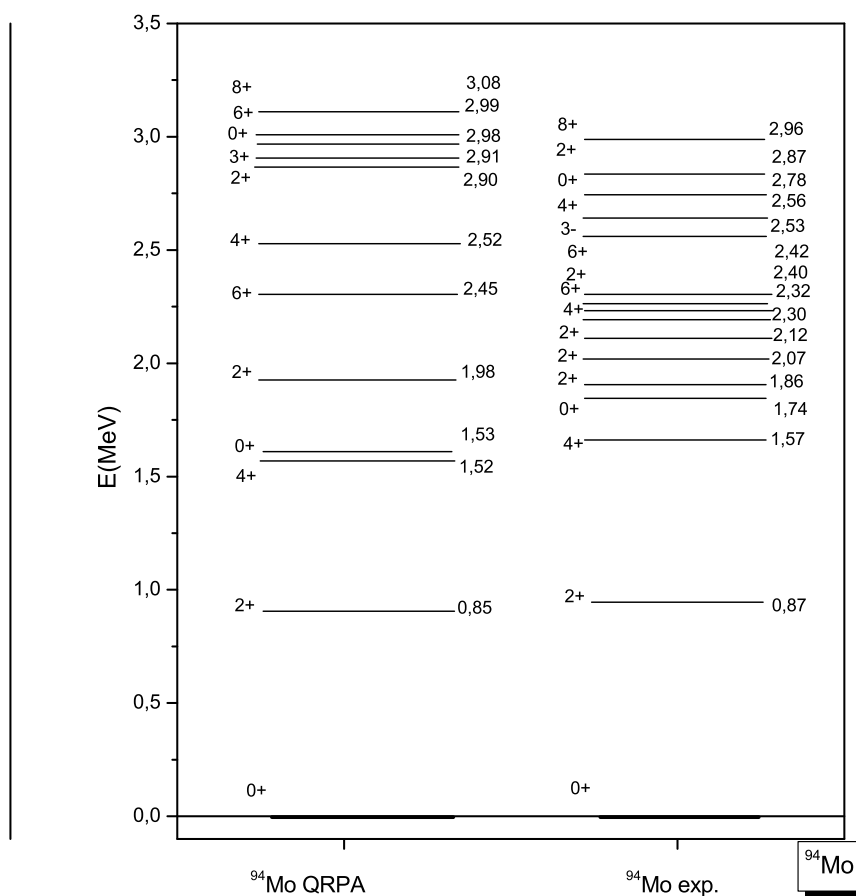


**FIGURE 1.** Comparison of experimental(left) and theoretical (right)low-energy spectra of  $^{94}\text{Mo}$  nucleus. The theoretical results are obtained by using the QRPA method.

## RESULTS

In this work we have performed realistic state-by-state calculations for inelastic and elastic neutrino-nucleus scattering off the stable  $^{94}\text{Mo}$  isotope. Our calculations were performed in five steps: First the wave functions of the initial (the  $0^+$  ground state of the even-even nucleus) and the final states were calculated within the QRPA. The obtained wave functions were subsequently used to evaluate the required reduced one-body transition densities. Then, the double-differential cross section was calculated for each scattering angle ( $\theta$ ), neutrino energy ( $E_\nu$ ) and final state. In the next step, the differential cross section as a function of the scattering angle and neutrino energy was obtained by summing over all the (discrete) final states. Then, numerical integration techniques were used to calculate the total cross section  $\sigma(E_\nu)$  as a function of neutrino energy. In the last step the averaged cross section  $\langle\sigma\rangle$  was finally obtained by folding the cross section  $\sigma(E_\nu)$  with a two-parameter Fermi-Dirac distribution appropriate for

**TABLE 1.** Pairing gaps and the corresponding pairing strength parameters

<i>Nucleus</i>	$\Delta_{np}$	$\Delta_{pp}$	$g_{ph}$	$g_{pp}$
$^{94}\text{Mo}$	0.979	1.510	1.040	0.972

supernova neutrinos.

For the construction of the wavefunctions of the initial and final nuclear states we used the QRPA method. Both Fermi and Gamow-Teller like contributions of the polar vector and axial vector have been considered. A Coulomb corrected Woods-Saxon potential was used as field interaction and as two body residual interaction the Bonn-C meson exchange potential was utilized. Our model space consists of the following eleven active single particle levels:  $0f^{7/2}$ ,  $1p^{3/2}$ ,  $1d^{1/2}$ ,  $0f^{5/2}$ ,  $0g^{9/2}$ ,  $1d^{5/2}$ ,  $2s^{1/2}$ ,  $1d^{3/2}$ ,  $0g^{7/2}$ ,  $0h^{11/2}$ ,  $0h^{9/2}$  (up to  $4\hbar\omega$  major harmonic oscillator shells).

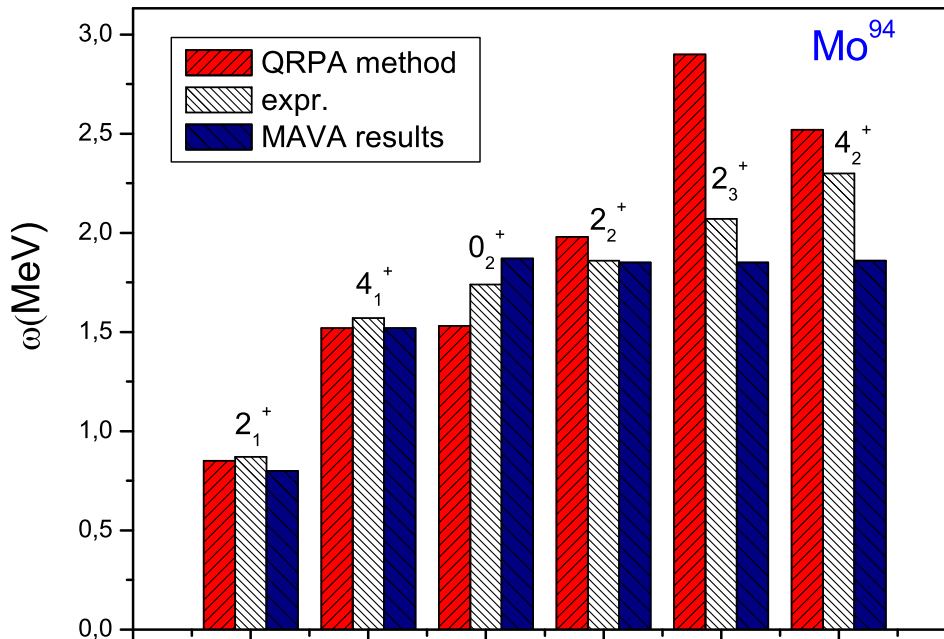


**FIGURE 2.** Excitation energies for the multipole states  $J^\pi = 2_1^+$ ,  $J^\pi = 4_1^+$  and  $J^\pi = 6_1^+$  of the  $^{94}\text{Mo}$  nucleus. Our theoretical results are compared with the experimental results as well as theoretical results obtained by the MAVA method

At the BCS level, the values of the pairing parameters for protons ( $g_{pair}^p$ ) and neutrons ( $g_{pair}^n$ ) which reproduce the pairing gaps in the usual way [7] was found to be  $g_{pair}^p = 0.972$  and  $g_{pair}^n = 1.040$ . By solving the QRPA equations the strength parameters for the particle-hole channel,  $g_{ph}$  and the particle-particle channel,  $g_{pp}$  were fixed so as the

lowest lying excitation energies to be reproduced. The above parameters get values in the ranges shown in Table 1. The evaluation of these strength parameters was obtained separately for each set of multiple states. By using the above parameters we produced the low-lying energy spectrum, shown in Figure 1, where this spectrum was compared to that given by experiment.

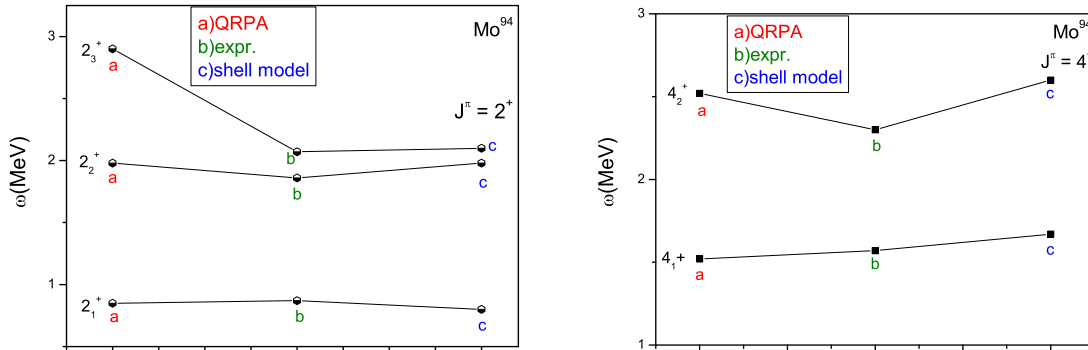


**FIGURE 3.** Excitation energies for the multipole states  $J^\pi = 2^+$  and  $J^\pi = 4^+$  of the  $^{94}\text{Mo}$  isotope. Our theoretical results are compared with the experimental results and results obtained by using the shell model method.

In Figure 2 we show the excitation energies of the multipole states  $J^\pi = 2_1^+$ ,  $J^\pi = 4_1^+$  and  $J^\pi = 6_1^+$  by using the QRPA method. In the low energy spectra our results are in good comparison with the experimental ones. In Figure 3 the excitation energies of the  $J^\pi = 2^+$  and  $J^\pi = 4^+$  states are illustrated. The obtained results are compared to the experimental results and those obtained by using the shell model method.

In the next step of our research we proceeded with the calculation of the cross sections. The primary results refer to the double differential cross sections of Eq.(2). Total differential cross sections were evaluated by summing over partial rates for various sets of multipole states included in our truncated model space up to  $J^\pi = 8^+$ . For integrated (total) cross-sections we used numerical integration techniques (Gauss method) to integrate the aforementioned differential cross sections [8]. From our results, shown in Table 2, one could conclude that the total cross sections are large at low energies. For higher neutrino energies, ( $\epsilon_i > 80$  MeV) the total cross sections are dramatically decreased [9, 10, 11, 12, 13, 14].

## SUMMARY AND CONCLUSIONS

In the present paper we employed the quasiparticle random-phase approximation (QRPA) to study the neutral-current neutrino-nucleus inelastic and elastic scattering cross sections. Our present results refer to the stable  $^{94}\text{Mo}$  isotope. The obtained energy spectra show a good agreement with experimental data.

The results for the contribution of the separate multipole sets of excited states have shown that for low-energy neutrino-scattering off  $^{94}\text{Mo}$  the cross sections are dominated by transitions to  $1^+$  states.

**TABLE 2.** Total cross sections (in  $10^{-40}cm^2$ ) for the neutral-current neutrino-nucleus reactions,  ${}^{94}Mo(\nu, \nu'){}^{94}Mo^*$ , calculated with QRPA method.

Initial Neutrino Energy $\varepsilon_i(MeV)$	Total reaction Cross Sections ${}^{94}Mo(\nu, \nu'){}^{94}Mo^*$
5	1.35(-2)
10	2.47(-2)
15	2.32(-1)
20	1.197(+0)
25	1.12(+1)
30	8.16(+1)
35	1.60(+1)
40	2.74(+2)
45	4.23(+2)
50	6.06(+2)
55	8.13(+3)
60	1.04(+3)
65	1.27(+4)
70	3.85(+4)
75	4.88(+4)
80	5.90(+4)
85	6.83(+4)
90	7.62(+4)
95	8.22(+4)
100	8.63(+4)

## ACKNOWLEDGMENTS

This research was supported by the ΠENEΔ No 03EΔ807 project of the General Secretariat for Research and Technology of the Hellenic Ministry of Development.

## REFERENCES

1. K. Langanke, *Rev. Mod. Phys.* **75**, (2003).
2. H. Ejiri, *Phys. Rep.* **338**, 265–351 (2000), and references therein.
3. W.C. Haxton, *Phys.Rev.Lett.* **60**, 768 (1988).
4. J.N. Bahcall and R.K. Ulrich, *Rev. Mod. Phys.* **60** (1988) 297.
5. V.Ch. Chasioti and T.S. Kosmas *Nucl. Phys. A* **829** (2009) 234.
6. T.S. Kosmas and E. Oset, *Phys. Rev. C* **53**, 1409–1415 (1996).
7. T.S. Kosmas, *Nucl Phys. A*, **683**, 443 (2001).
8. E. Kolbe and T.S. Kosmas, *Springer Trac. Mod. Phys.* **163**, 199–225 (2000).
9. K.G. Balasi, T.S. Kosmas, P.C. Divari and V.C. Chasioti, *Proc. of the Carp. Sum. Sch. of Phy.* **554-557** (2007).
10. K.G. Balasi, T.S. Kosmas, P.C. Divari and V.Ch. Chasioti, *AIP Conf. Proc.* **972** (2008) 554.
11. K.G. Balasi, T.S. Kosmas, P.C. Divari and H.Ejiri, *J. Phys. Conf. Ser.* **203** (2010) 012101.
12. K.G. Balasi, T.S. Kosmas, P.C. Divari, *AIP Conf. Proc.* **1180** (2009) 1.
13. K.G. Balasi, T.S. Kosmas, P.C. Divari, *Prog. Part. Nucl. Phys.* **64** (2010) 414.
14. K.G. Balasi, T.S. Kosmas, E. Ydrefords, *Nucl. Phys. A* **submitted** (2011) .